Original Research

Reduction in mitochondrial oxidative stress mediates hypoxia-induced resistance to cisplatin in human transitional cell carcinoma cells

Myung-Chul Kim [a,b,d]; **Sung-Hyun Hwang** [a,b]; **Yeseul Yang** [a,b]; **Na-Yon Kim** [a,b]; **Yongbaek Kim** [a,c,*]

[a] Laboratory of Clinical Pathology, College of Veterinary Medicine, Seoul National University, Seoul, The Republic of Korea
[b] BK21 PLUS Program for Creative Veterinary Science Research, College of Veterinary Medicine, Seoul National University, Seoul, The Republic of Korea
[c] Research Institute for Veterinary Science, College of Veterinary Medicine, Seoul National University, Seoul, The Republic of Korea
[d] Department of Pathology, Immunology and Laboratory Medicine, College of Medicine, University of Florida, Gainesville, FL, USA

Abstract

Tumor hypoxia is known to promote the acquisition of more aggressive phenotypes in human transitional cell carcinoma (TCC), including drug resistance. Accumulating evidence suggests that mitochondria play a central role in the chemoresistance of TCC. However, the role of mitochondria in the hypoxia-induced drug resistance in TCC remains elusive. The present study investigated the function of mitochondria in the drug resistance using a TCC cell line under hypoxic conditions. *In vitro* hypoxia (0.1% O_2, 48 h) was achieved by incubating TCC cells in air chamber. Mitochondrial events involving hypoxia-induced drug resistance were assessed. Hypoxia significantly reduced the cisplatin-induced apoptosis of TCC cells. Additionally, hypoxia substantially decreased the level of mitochondrial reactive oxygen species (ROS) generated by cisplatin treatment. Analogously, elimination of mitochondrial ROS significantly rescued cells from cisplatin-induced apoptosis. Hypoxia enhanced mitochondrial hyperpolarization, which was not related to ATP production or the reversal of ATP synthase activity. The mitochondrial DNA (mtDNA) amplification efficiency data illustrated that hypoxia significantly prevented oxidative damage to the mitogenome. Moreover, transmission electron microscopy revealed that cisplatin-induced disruption of the mitochondrial ultrastructure was abated under hypoxic conditions. Notably, depletion of mtDNA by ethidium bromide abrogated hypoxia-induced resistance to cisplatin. Taken together, the present study demonstrated that TCC cells exposed to hypoxic conditions rendered mitochondria less sensitive to oxidative stress induced by cisplatin treatment, leading to enhanced drug resistance.

Neoplasia (2021) 23, 653–662

Introduction

Tumor hypoxia is a hallmark of almost all types of cancers [1] and is significantly associated with tumor aggressiveness [2]. Enhancement of drug resistance by tumor hypoxia is a major obstacle to effective therapy in cancer patients [3]. The mechanisms responsible for hypoxia-induced drug resistance are multifactorial and complex and differ depending on the type of cells, drugs and experimental settings [4, 5]. Hypoxia-inducible factor alpha (HIF-1α) is considered a master regulator of hypoxia-induced phenotypic changes, including drug resistance [5].

Urinary bladder cancer is a common disease and is the tenth most common malignancy worldwide [6]. Approximately 81,400 new bladder cancer cases were diagnosed in the United States in 2020 [7]. Transitional cell carcinoma (TCC) is the most common type of urinary bladder cancer

[8]. TCC tumors are histologically divided into nonmuscle-invasive and muscle-invasive tumors based on the invasion of the lamina propria [8]. The 5-y overall survival rate of patients with nonmetastatic muscle-invasive tumors is 36 to 48% [8]. The overall prognosis of metastatic bladder cancer is poor, with a survival of 13 to 15 mo from diagnosis [8]. Most patients with muscle-invasive and advanced disease begin to receive neoadjuvant chemotherapy before surgical intervention or radiation, and cisplatin is one of the standard first-line chemotherapeutics [8]. Muscle-invasive tumors can be aggressive and metastasize after radical cystectomy and systemic chemotherapy [8]. The major barrier to effective chemotherapy in TCC patients is acquired drug resistance [9]. Published studies have shown that hypoxia is strongly associated with poor prognosis and the resistance to anticancer drugs in bladder cancer patients [10-12].

Mitochondria are double-membraned intracellular organelles that participate in a variety of physiological processes, such as ATP production, apoptosis, and reactive oxygen species (ROS) generation [13]. The genome of mitochondria, mitochondrial DNA (mtDNA), encodes 13 polypeptides essential for respiration and oxidative phosphorylation [14]. The mitochondrial respiratory chain is closely associated with the modulation of apoptosis and generation of ROS [15]. Mitochondria have been proposed as a feasible target for cancer therapy [16]. In drug-resistant bladder cancer cells, antiapoptotic mitochondrial proteins are highly activated [17, 18]. TCC cells acquire cisplatin resistance via HIF-1α induction and down-regulation of proapoptotic mitochondrial gene [17]. In the present study, we hypothesized that mitochondrial events are critical for hypoxia-induced drug resistance in TCC cells.

In this study, we demonstrated that mitochondrial events are critical for the development of hypoxia-related drug resistance in the T24 cell line, a cell line from a patient with high-grade and invasive urinary bladder cancer. Our data suggest that targeting the mitochondrial genome may enhance therapeutic efficacy in TCC patients.

Materials and methods

Cell culture and reagents

The T24 cell line (T24) was kindly provided by Dr. Jablons (University of California, San Francisco). Short tandem repeat analysis by Korean Cell Line Bank (Seoul, South Korea) verified the identity of the T24 cell line. The T24 cell line was maintained in RPMI 1640 medium (HyClone, Fisher Scientific, Logan, UT, USA) supplemented with 10% FBS (HyClone, Fisher Scientific). The T24 cell line was determined to be free of mycoplasma contamination by using an e-Myco Mycoplasma PCR Detection Kit (e-Myco, iNtRON Biotechnology, Sungnam, Korea). Cisplatin was purchased from Dong-A Pharmaceutical Co., Ltd. Unless stated otherwise, T24 cells were treated with 10 μM cisplatin for 48 h. Ethidium bromide (EtBr), uridine, 3-(4,5-dimethylthiazol-2-yl)-2,5-diphenyl tetrazolium bromide (MTT), N-acetyl cysteine (NAC), and oligomycin were purchased from Sigma-Aldrich (St. Louis, MO, USA). Hypoxic conditions (0.1% O_2/5% $_{CO-2}$/94.9% N_2) were established by using an air chamber (Billups-Rothenberg Inc., Del Mar, CA, USA). T24 cells were exposed to the hypoxic conditions for 48 h.

Measurement of cell viability

Cell viability was determined by the MTT assay as described previously [19]. The absorbance was determined at 570 nm with a microplate reader (Gen5, Epoch Bio Tek, Winooski, VT, USA). The absorbance of T24 cells under normoxia was set as 100%, and all other measurements are expressed as the percentage relative to the value of the control cells and the standard deviation (SD).

Apoptosis assay

The apoptosis rate was measured by the annexin V staining method as previously described [19]. Annexin V- or propidium iodide (PI)-positive cells identified by flow cytometric analysis were considered to be apoptotic cells, and the mean percentage of apoptotic cells and SD are presented. Flow cytometric analysis was performed using the FACS system (Becton Dickinson, San Jose, CA, USA). Flowing software version 2.5.1 (www.flowingsoftware.com) was used to calculate the mean fluorescence intensities of the fluorochromes in arbitrary units (a.u.s).

Measurement of DNA fragmentation

T24 cells in the log phase of growth were treated with cisplatin under normoxic or hypoxic conditions. The cells were harvested and fixed with cold 70% ethanol at -20°C for 2 h. After washing with PBS, the cells were incubated with 500 μL PI/RNase staining buffer (BD Pharmingen, BD Biosciences) for 15 min at room temperature. The cell suspensions were analyzed by flow cytometry to determine the cellular DNA content. Cells in the sub G1 phase were considered to have fragmented DNA. The results are presented as the percentage of cells with fragmented DNA using Modfit LT software (Verity Software House Inc., Topsham, Maine, USA).

Measurement of the mitochondrial membrane potential

The mitochondrial membrane potential (MMP) was evaluated by the JC-1 assay (Molecular Probes, Fisher Scientific) according to the manufacturer's instructions. After exposure to cisplatin and/or hypoxia, T24 cells were subjected to staining with JC-1 at a final concentration of 2 μM at 37°C for 30 min in the dark. T24 cells were harvested, resuspended, and analyzed by flow cytometry. The MMP was calculated by determining the ratio of JC-1 aggregates to monomers. T24 cells incubated with JC-1 in the presence of carbonyl cyanide 3-chlorophenylhydrazone (CCCP) at a concentration of 50 mM were used as positive controls for dissipation of the membrane potential. The JC-1 ratio of untreated control cells under normoxia was considered 100%, and the values for all other groups are expressed as the percentage relative to the value of the control cells and the SD. To determine the mode of action of ATP synthase, T24 cells were incubated with JC-1 in the presence of oligomycin, a pharmacologic inhibitor of ATP synthase.

Semiquantitation of intracellular ATP levels

Cellular ATP levels were measured in a semiquantitative manner using an ATP-based CellTiter-Glo Luminescent Cell Viability Kit (Promega, Madison, WI,USA) according to the manufacturer's instructions. Briefly, Cell Titer-Glo reagent was added to T24 cells that had been treated with cisplatin under either normoxia or hypoxia. The luminescence values were determined using a luminescent plate reader (Thermo Lab system, Franklin, MA, USA).

Measurement of oxidative stress

T24 cells exposed to cisplatin or hypoxia were further incubated with 2 μM CM-H_2-DCFDA (Molecular Probes), a cellular hydrogen peroxide (H_2O_2) indicator, for 30 min; 2 μM MitoSox Red (Molecular Probes), a mitochondrial superoxide indicator, for 15 min; and 5 μM Mito PY1 (Sigma-Aldrich), a mitochondrial H_2O_2 indicator, for 30 min at 37°C in the dark. After being harvested, the cells were suspended in PBS and subjected to flow cytometry to measure the changes in ROS levels.

Measurement of mtDNA damage and depletion of mtDNA

Damage to mtDNA was measured by assessing the amplification efficiency of a large fragment of mtDNA relative to a short amplicon of mtDNA in

Table 1

Primer sequences used for measurement of MtDNA copy number and amplification efficiency in this study.

Target	Direction	Primer sequences (5′ to 3′)
ND1	Forward	AACATACCCATGGCCAACCT
	Reverse	GGCAGGAGTAATCAGAGGTG
ND2	Forward	TAAAACTAGGAATAGCCCCC
	Reverse	TTGAGTAGTAGGAATGCGGT
ND3	Forward	CACAACTCAACGGCTACATA
	Reverse	TTGTAGTCACTCATAGGCCA
ND4	Forward	TCTTCTTCGAAACCACACTT
	Reverse	AAGTACTATTGACCCAGCGA
ND6	Forward	TCCGTGCGAGAATAATGATG
	Reverse	ATAACCTATTCCCCCGAGCA
Cytochrome b	Forward	AGTCCCACCCTCACACGATTC
	Reverse	ACTGGTTGTCCTCCGATTCAGG
COXI	Forward	ACACGAGCATATTTCACCTCCG
	Reverse	GGATTTTGGCGTAGGTTTGGTC
COXII	Forward	ATCAAATCAATTGGCCACCAATGGTA
	Reverse	TTGACCGTAGTATACCCCCGGTC
COXIII	Forward	ACATCCGTATTACTCGCATC
	Reverse	AACCACATCTACAAAATGCC
ATPase 6	Forward	CTCACCAAAGCCCATAAA
	Reverse	AGGCGACAGCGATTTCTA
ATPase 8	Forward	TGCCCCAACTAAATACTACC
	Reverse	ATGAATGAAGCGAACAGATT
tRNA-Leu (UUA)	Forward	CACCCAAGAACAGGGTTTGT
	Reverse	TGGCCATGGGTATGTTGTTA
8.9 kb mitochondria fragment, entire	Forward	TCTAAGCCTCCTTATTCGAGCCGA
	Reverse	TTTCATCATGCGGAGATGTTGGATGG
8.9 kb mitochondria fragment, beginning	Forward	CCCCACAAACCCCATTACTAAACCCA
	Reverse	TTTCATCATGCGGAGATGTTGCATGG
B2-microglobulin	Forward	TGCTGTCTCCATGTTTGATGTATC
	Reverse	TCTCTGCTCCCCACCTCTAAGT

which various types of DNA lesions slow down or block the progression of DNA polymerase [20]. Total DNA was extracted using the DNeasy Blood and Tissue Kit (Qiagen, Valencia, CA, USA) according to the manufacturer's instructions. The DNA quality and quantity were determined using a Nanodrop 1000 spectrophotometer (Nanodrop Technologies, Wilmington, DE, USA). The long mtDNA fragment was amplified using the GoTaq Long PCR Master Mix kit (Promega) according to the manufacturer's instructions. Ten nanograms of genomic DNA were subjected to long PCR (94°C for 2 min 20 s and 19 cycles of 65°C for 9 min and 72°C for 10 min) to synthesize an 8.9 kb mitochondrial fragment [20]. After gel electrophoresis, the PCR products were quantified using ImageJ software (ImageJ, US National Institutes of Health, Bethesda, MD; http://imagej.nih.gov/ij/). To account for differences in mtDNA copy number between samples, long PCR amplification values were normalized to the geometric mean by combining the levels of COXI and tRNA-Leu (UUA), and the short PCR result of the start site of the corresponding 8.9 kb mitochondrial genome. The mtDNA copy number was normalized to that of nuclear β2-microglobulin. The mitochondrial short fragments were amplified by quantitative real-time PCR based on the $\Delta\Delta$Ct method [19]. Ten nanograms of total genomic DNA were subjected to PCR (95°C for 10 min and 45 cycles of 95°C for 10 s, 60°C for 15 s, and 72°C for 30 s). Each reaction mixture consisted of

10 μL of SYBR Green Mix, 1 μL of each 10 μM primer, and 7 μL of DNA in RNase-free water.

T24 cells were cultured in the presence of 50 ng/mL EtBr and 50 μg/mL uridine for more than 4 wk as previously described [21]. The mtDNA-depleted T24 cells, also referred to as $\rho°$ cells, were maintained treated with EtBr and uridine throughout the entire experiment. Depletion of mtDNA in T24 cells was verified by PCR analysis using mtDNA-specific primers as described above. The primer sequences used in this study are listed in Table 1.

Transmission electron microscopy

The ultrastructure of T24 cells was examined as previously described [22]. Briefly, T24 cells were harvested and fixed with Karnovsky's solution overnight. After washing with 0.05 M sodium cacodylate, the cells were postfixed with 2% osmium tetroxide for 2 h. The cells were subsequently dehydrated in an ascending alcohol series and finally embedded in Spurr's resin. After complete ultrathin sectioning with an EM UC-7 Ultramicrotome (Leica Microsystems, Vienna, Austria), the T24 cells were examined using a transmission electron microscope (LIBRA 120, Carl Zeiss, Jena, Germany).
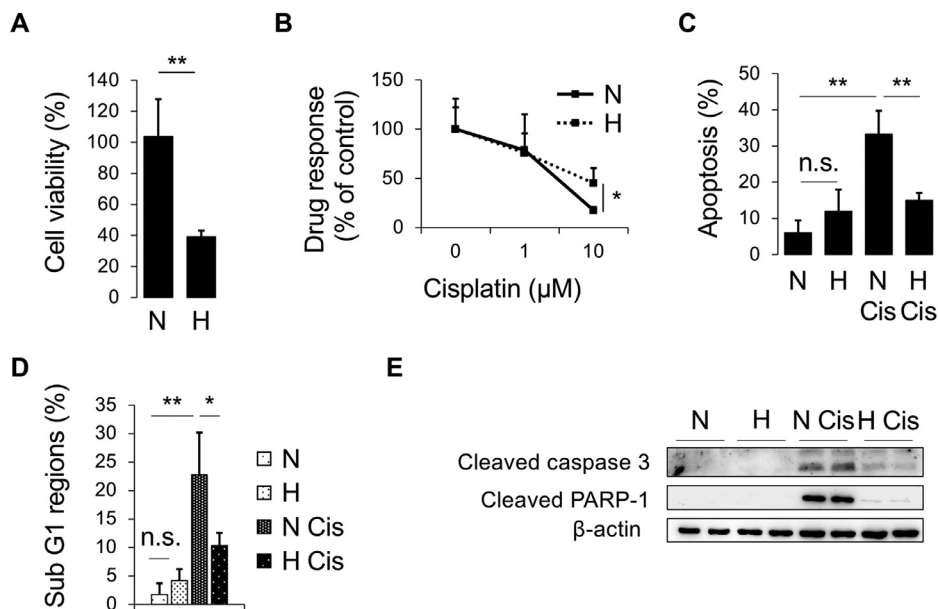
Fig. 1. Hypoxia decreases cell viability but induces cisplatin resistance through inhibition of T24 cell apoptosis. (A) MTT assay. T24 cells exposed to hypoxia show a significant reduction in cell viability ($n = 6$). (B) MTT assay. Drug sensitivity to 10 μM cisplatin is significantly decreased in T24 cells exposed to hypoxia compared to cells exposed to normoxia ($n = 4$). (C) Apoptosis assay. Cisplatin dramatically increases apoptosis of T24 cells. Hypoxia tends to increase apoptosis and significantly inhibits cisplatin-induced apoptosis of T24 cells ($n = 6$). (D) DNA fragmentation assay. Cisplatin causes DNA fragmentation in T24 cells. Hypoxia significantly decreases the percentage of sub G1 populations generated by cisplatin ($n = 3$). (E) Western blot analysis. Hypoxia decreases cisplatin-induced caspase-3 and PARP-1 expression. β-actin was used for the loading control. The P value was calculated by Student's t-test or one-way ANOVA followed by the Bonferroni post hoc test. Abbreviations: Cis, cisplatin; H, hypoxia (48 h); N, normoxia; n.s., not significant. * $P < 0.05$ and ** $P < 0.01$.

Western blot analysis

The Western blot assay was performed as previously described in detail [19]. GAPDH, β-actin (Santa Cruz Biotech, CA, USA), cleaved Caspase-3 (Cell Signaling, Beverly, MA, USA), γ-H2AX, and cleaved PARP-1 (Abcam, Cambridge, UK) antibodies were used. β-Actin or GAPDH was used as a loading control. The protein bands were visualized using enhanced chemiluminescence detection reagents (Advansta, Menlo Park, CA, USA) on an LAS system (Las 4000 mini, GE Health Care, USA). Densitometric analysis was performed using ImageJ software.

Statistical analysis

All data are presented as the means $\pm$ SD. The bars in the graphs represent at least 3 biological replicates, and representative experimental results are presented. Statistical analyses were performed with Microsoft Excel (Microsoft, Redmond, WA, USA) and SPSS Statistics for Windows (SPSS Inc, Chicago, IL, USA). Differences were considered statistically significant when the P value was less than 0.05: *$P < 0.05$ and **$P < 0.01$.

Results

Hypoxia increased resistance to cisplatin through inhibition of apoptosis

T24 cells exposed to hypoxia showed a significant reduction in cell viability (Fig. 1A). However, T24 cells were less sensitive to 10 μM cisplatin under hypoxic conditions than under normoxic conditions (Fig. 1B). Since cisplatin is a potent inducer of apoptosis of T24 cells [23], we investigated the apoptosis rate of T24 cells under hypoxic conditions. Cisplatin dramatically induced apoptosis of T24 cells under normoxic conditions. Hypoxia also induced apoptosis of T24 cells, but the effect was not statistically significant

(Fig. 1C). When T24 cells were treated with cisplatin under hypoxia, apoptosis was significantly reduced (Fig. 1C). Parallel measurements of DNA fragmentation also revealed that hypoxia induced a significant reduction in cisplatin-induced sub G1 populations, suggesting DNA hypoploidy indicative of late apoptosis (Fig. 1D). Western blot analysis showed that hypoxia inhibited the cleavage of caspase 3 and formation of PARP-1 proteolytic fragments induced by cisplatin (Fig. 1E).

Following cisplatin treatment, hypoxia-induced mitochondrial hyperpolarization not associated with respiratory chain dysfunction or ATP production in T24 Cells

The mitochondrial membrane potential is integral to mitochondrial function [13]. Cisplatin significantly altered the MMP in T24 cells (Fig. 2A). Hypoxia induced mitochondrial hyperpolarization in T24 cells, which was further enhanced by cisplatin treatment (Fig. 2A). Since severely damaged cells with electron transfer chain (ETC) dysfunction can exhibit mitochondrial hyperpolarization via the reversal of ATP synthase activity [24], we investigated the mode of action of the respiratory subunit using oligomycin, a specific inhibitor of ATP synthase (Fig. 2B). As shown in Figure 2C, the cisplatin-treated hypoxic T24 cells increased the MMP when cotreated with oligomycin and JC-1, indicating that ATP synthase operated in forward mode and that H$^+$ flowed from the mitochondrial intermembrane space into the matrix. Next, we examined whether hyperpolarized mitochondria are functionally related to ATP production. Cisplatin treatment decreased ATP levels in T24 cells independent of oxygen concentration (Fig. 2D). These data indicate that hyperpolarization of mitochondria is not directly coupled with ATP production or energy metabolism in T24 cells.
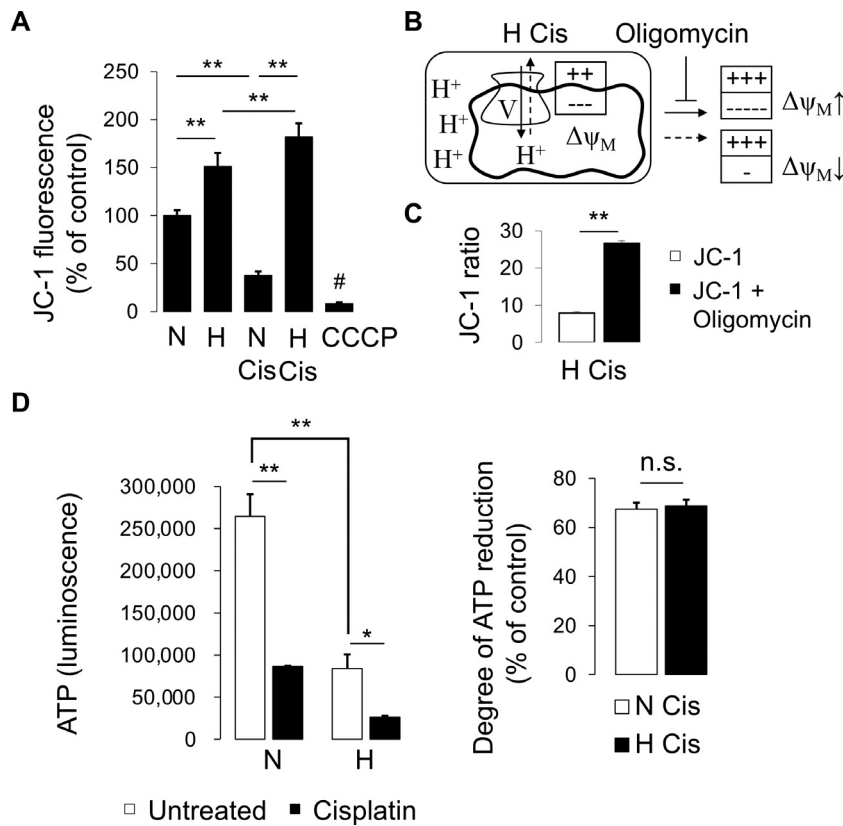
Fig. 2. Hypoxia induces mitochondrial hyperpolarization unrelated to ATP generation and reverses the mode of action of F_1F_0 ATP synthase in T24 cells. (A) JC-1 assay. Cisplatin significantly decreases the mitochondrial membrane potential (MMP). Hypoxia increases the MMP. Hypoxia induces constant mitochondrial hyperpolarization when cisplatin is administered. CCCP was used for the control of membrane dissipation ($n = 3$). (B) Mitochondrial ATP synthase could have either a forward (solid line) or reverse (dotted line) mode of action. Oligomycin determines the mode of action of ATP synthase by inhibiting H^+ flow and changing the MMP in the cisplatin-treated hypoxic T24 cells. Bold line: inner membrane of mitochondria, $\Delta\psi_M$: MMP, V: ATP synthase. Mitochondrial complex I, II, III, and IV are omitted. (C) JC-1 assay shows that oligomycin at a concentration of 50 μM enhances MMP in cisplatin-treated T24 cells under hypoxia ($n = 3$). (D) Intracellular ATP measurement. Hypoxia or cisplatin significantly reduces the intracellular ATP content in T24 cells ($n = 3$). The degree of ATP reduction is not different between normoxic and hypoxic T24 cells. The P value was calculated by one-way ANOVA followed by the Bonferroni post hoc test. #, significant differences compared to the untreated control group. Abbreviations: Cis, cisplatin; H, hypoxia (48 h); N, normoxia; n.s., not significant. * $P < 0.05$ and ** $P < 0.01$.
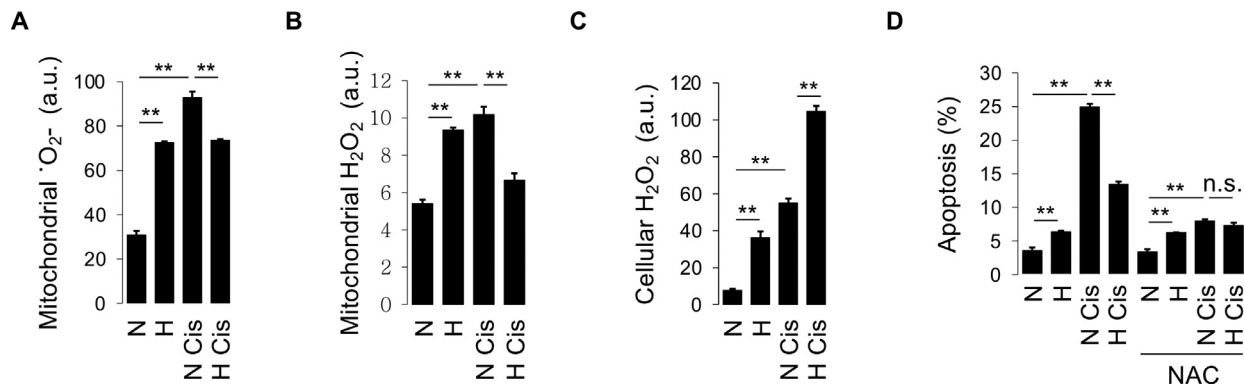

Fig. 3. Hypoxia mitigates mitochondrial oxidative stress induced by cisplatin in T24 cells. Cytometric assessment of ROS levels using fluorochromes. Cisplatin markedly increases cytosolic and mitochondrial ROS levels in T24 cells. Hypoxia significantly inhibits cisplatin-induced mitochondrial oxidative stress, as determined by the measurement of $O_2\bullet^-$ (A) and H_2O_2 (B) levels in T24 cells ($n = 3$). (C) Hypoxia enhances cytosolic ROS generation induced by cisplatin in T24 cells ($n = 4$). (D) Apoptosis assay. The antioxidant agent NAC at a concentration of 10 mM inhibits cisplatin-induced apoptosis in T24 cells ($n = 3$). The P value was calculated by one-way ANOVA followed by the Bonferroni post hoc test. Abbreviations: Cis, cisplatin; H, hypoxia (48 h); N, normoxia; n.s., not significant. * $P < 0.05$ and ** $P < 0.01$.
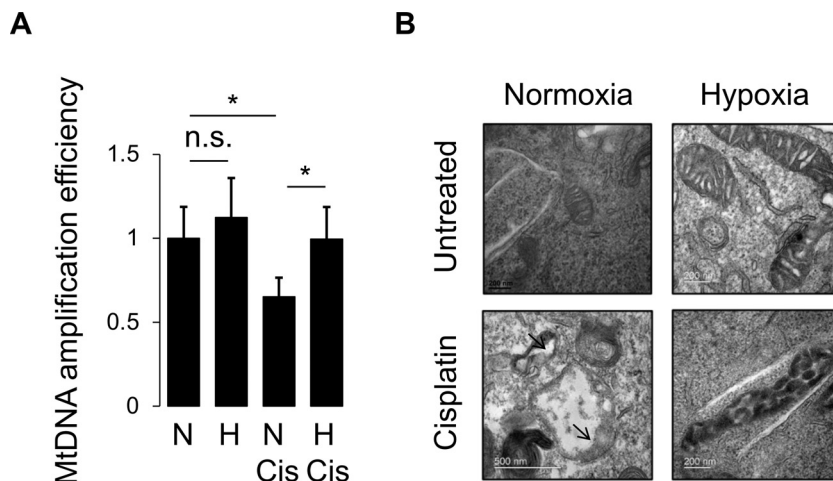
Fig. 4. Hypoxia protects mtDNA and the ultrastructure of mitochondria from the effect of cisplatin in T24 cells. (A) Cisplatin significantly decreases the amplification efficiency of mtDNA. Hypoxia prevents the reduction in mtDNA amplification efficiency induced by cisplatin ($n = 3$). (B) Transmission electron microscopy revealed that cisplatin induces morphologic changes in mitochondria characterized by membrane disruption and degradation of internal structures. Arrow indicates the degraded inner membrane structures of mitochondria. Hypoxia prevents structural damage to mitochondria induced by cisplatin and causes mitochondrial hypercondensation in T24 cells. The P value was calculated by one-way ANOVA followed by the Bonferroni post hoc test. Abbreviations: Cis, cisplatin; H, hypoxia (48 h); N, normoxia; n.s., not significant. * $P < 0.05$ and ** $P < 0.01$.

Hypoxia alleviated cisplatin-induced mitochondrial oxidative stress

Mitochondria have a respiratory ETC that is a substantial source of ROS and oxidative stress induced by cisplatin treatment [13]. Fluorometric analysis revealed that cisplatin enhanced the generation of mitochondrial superoxide and H_2O_2 in T24 cells. Hypoxia alone also increased mitochondrial ROS production in T24 cells (Fig. 3A and 3B). However, hypoxia significantly decreased the production of mitochondrial ROS induced by cisplatin (Fig. 3A and 3B). On the other hand, when the cellular ROS levels were measured by CM-H_2-DCFDA, cisplatin-induced oxidative stress was not mitigated by hypoxia (Fig. 3C). Treatment with an ROS scavenger protected T24 cells from cisplatin-induced oxidative stress (Fig. 3D).

Hypoxia protected T24 cells from cisplatin-induced oxidative damage to mtDNA and mitochondrial ultrastructure changes

Mitochondrial oxidative stress affects the integrity of mtDNA and structural components [25]. To determine whether hypoxia contributes to protecting mitochondria from cisplatin-induced oxidative stress, we assessed mtDNA damage by measuring the mtDNA amplification efficiency [20]. As shown in Fig. 4A, cisplatin significantly reduced the mtDNA amplification efficiency, suggesting the presence of oxidative lesions in the mtDNA. Hypoxia itself did not alter the amplification efficiency in T24 cells, but it significantly enhanced the impact of cisplatin on the mtDNA amplification efficiency.

These findings were further supported by ultrastructural evaluation, which showed that hypoxia alleviated the mitochondrial degradation induced by cisplatin (Fig.e 4B). Unlike the well-conserved cristae of the mitochondria of the control cells, the mitochondria of the cisplatin-treated T24 cells exhibited vesicles, a swollen matrix and electrolucent, disorganized cristae. Under hypoxic conditions, the morphology of the mitochondria was close to normal, although a few mitochondria had either a partially swollen or electron-dense matrix in a spherical, bean, or tubular shape. Mitochondrial hypercondensation was conspicuous in cisplatin-treated cells under hypoxia. Additionally, neither rarefaction of the matrix nor degeneration of internal cristae was observed in these cells.

Depletion of mtDNA helped overcome hypoxia-induced drug resistance in T24 cells

To determine whether mitochondria were directly involved in hypoxia-induced drug resistance in T24 cells, we depleted mtDNA. A total of 11 mitochondrial genes encoding proteins of the ETC as well as 2 noncoding areas of the mtDNA were assessed. Long-term exposure of T24 cells to a low dose of EtBr resulted in depletion of mtDNA (Fig. 5A). $\rho°$ cells showed a complete collapse of MMP (Fig. 5B), a profound decrease in mitochondrial ROS generation (Fig. 5C), and a significant reduction in cellular ATP levels (Fig. 5D). Moreover, the mitochondria of $\rho°$ cells exhibited disorganized cristae and a swollen matrix (Fig. 5E).

Cisplatin significantly enhanced apoptosis of both parental and ρ^0 cells, and hypoxia alone did not affect apoptosis. Unlike parental cells, which showed drug resistance under hypoxia, ρ^0 cells did not exhibit hypoxia-induced drug resistance (Fig. 5F). Fluorometric analysis showed that hypoxia enhanced cisplatin-induced ROS generation in $\rho°$ cells (Fig. 5G). At the molecular level, the expression levels of caspase 3 and PARP-1 remained unchanged in cisplatin-treated ρ^0 cells under normoxic and hypoxic conditions (Fig. 5H). Intriguingly, hypoxia reduced the expression of γ-H2AX, a marker of nuclear DNA double-strand breaks, in both parental and $\rho°$ cells after cisplatin treatment (Fig. 5H).

Discussion

Clinical and biological evidence indicates that hypoxia occurs in TCC [26, 27]. Hypoxia promotes the acquisition of more aggressive behaviors by TCC cells, including drug resistance [28]. Thus far, the role of mitochondria in hypoxia-induced drug resistance is poorly understood. Herein, by depleting mtDNA, we illustrated that mitochondria are the key players in hypoxia-induced drug resistance in TCC cells. The present study suggests that targeting mtDNA may contribute to improving drug efficacy in TCC patients. A graphical summary of the proposed mechanism is presented in Figure 6.

Tumor cells exposed to hypoxia have reduced mitochondrial activity, which is associated with enhanced drug resistance [29-32]. In our study, hypoxia decreased mitochondrial activity and induced mitochondrial
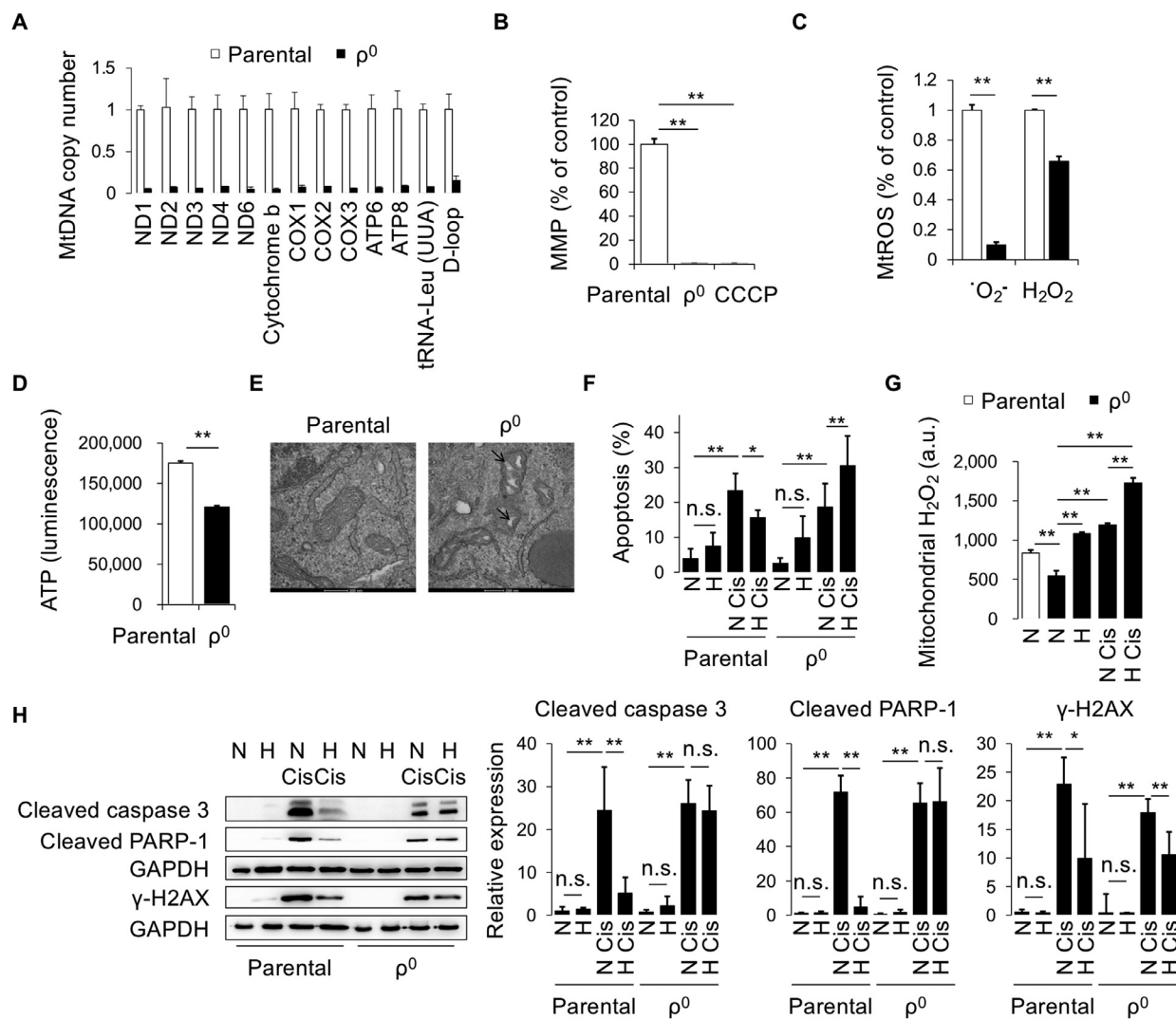
Fig. 5. MtDNA depletion abrogates hypoxia-induced cisplatin resistance through disrupting mitochondrial integrity in T24 cells. (A) Establishment and characterization of mtDNA-depleted T24 cells. Long-term treatment of T24 cells with EtBr significantly depletes mtDNA ($n = 2$). Compared with parental cells, T24 cells with depleted mtDNA show a significant reduction in the MMP ($n = 3$) (B), mitochondrial ROS production ($n = 3$) (C), and intracellular ATP levels ($n = 5$) (D). CCCP was used for the control of membrane dissipation. (E) Transmission electron microscopy revealed that mtDNA depletion causes swelling of the matrix and disorganization of cristae in mitochondria, indicated by arrow. (F) mtDNA depletion reverses resistance to apoptosis induced by hypoxia in T24 cells treated with cisplatin ($n = 4$). (G) Western blot analysis. Hypoxia enhances mitochondrial H_2O_2 generation in ρ^0 T24 cells induced by cisplatin ($n = 3$). (H) mtDNA depletion abrogates hypoxia-induced apoptosis resistance to cisplatin in T24 cells. Hypoxia significantly reduces the increase in γ-H2AX expression induced by cisplatin in both parental and ρ^0 T24 cells ($n = 5$). GAPDH was used for the loading control. The P value was calculated by Student's t-test or one-way ANOVA followed by the Bonferroni post hoc test. Abbreviations: Cis, cisplatin; H, hypoxia (48 h); N, normoxia; n.s., not significant. * $P < 0.05$ and ** $P < 0.01$.

hyperpolarization in TCC cells. Similar changes in mitochondria have been reported to be associated with acquired cisplatin resistance in other cancers [33]. Moreover, we showed that hypoxia protected TCC cells from the effects of cisplatin, including changes in mitochondrial structure, oxidative stress, and mtDNA damage. There is a direct correlation between fewer mtDNA lesions and greater drug resistance [34, 35]. It has been noted that the mitochondrial ultrastructure is protected in cisplatin-resistant cancer cells with hyperpolarized mitochondria [36]. Hyperpolarization of mitochondria is closely associated with chronic inhibition of complex I [37]. Reducing oxidative stress by modulating the mitochondrial ETC complex is directly associated with drug resistance [38-41]. Intriguingly, the fact that mitochondrial hyperpolarization is accompanied by cytosolic ROS accumulation when oxidative stress is reduced in mitochondria is consistent

with our results [42, 43]. These data may imply that the mechanism by which hypoxia induces drug resistance may be associated with redox regulation via the mitochondrial ETC system. Indeed, there is evidence that hypoxia rearranges distinct subunits of the respiratory chain to alter mitochondrial ROS formation in cancer cells [44]. Remodeling of the respiratory complex potentially restricts excessive ROS generation after drug treatment [38-40]. Abrogation of the response to hypoxia and impairment of apoptosis resistance to oxidative stress following respiratory defects due to either mtDNA mutation or misassembly of mitochondrial ETC subunits strongly supports our findings [45, 46]. Thus, we speculate that hypoxia may act as a modulator of the respiratory electron transfer system, which minimizes cisplatin-induced ROS generation in T24 cells. The precise mechanism by which hypoxia regulates redox homeostasis via the mitochondrial
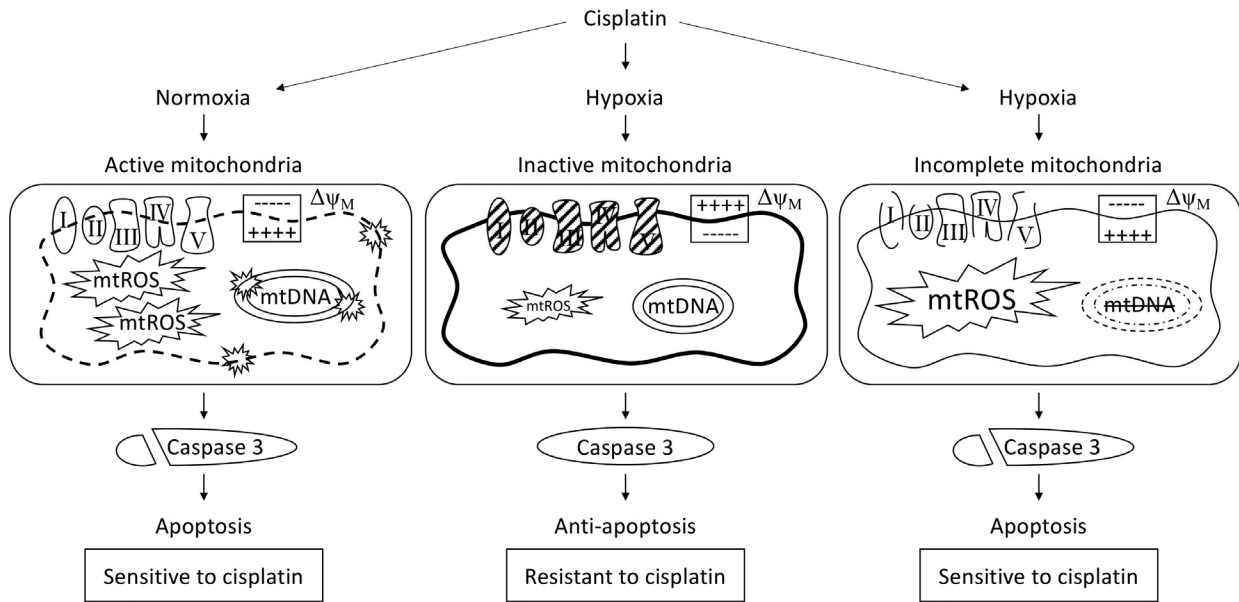
Fig. 6. The proposed mechanism underlying hypoxia-induced cisplatin resistance in T24 cells. The intact mitochondrial respiratory chain complex is presented by a solid line. The upward diagonal pattern indicates mitochondrial respiratory inhibition under hypoxic conditions. The dashed line indicates mitochondria with an incomplete respiratory chain due to mtDNA depletion. The dotted line on the inner membrane of mitochondria represents damage induced by cisplatin. The protective effect of hypoxia on the mitochondrial inner membrane is indicated by the bold line.

respiratory chain and thereby induces drug resistance warrants further study.

Modulating mitochondrial activity has been proposed as a potential strategy to overcome hypoxia-induced drug resistance in multiple cancer types [38-41, 47]. Our results provide support for this hypothesis and further suggest that targeting mtDNA can improve the treatment of hypoxia in TCC. Thus, delivering drugs to mitochondria to selectively target mtDNA could be a promising approach to treat patients with TCC and other cancers [48]. Therapeutic efficacy of mtDNA targeting could be augmented by the use of lipophilic cations-based drugs that preferentially accumulate within hyperpolarized mitochondria in hypoxic cancer cells [49].

There are potential limitations in the present study. We only tested our hypothesis by *in vitro* assays using single cell line. Thus, further studies are warranted to determine if our conclusions are applicable to other TCC cell lines and also can be reproduced by *in vivo* tumor models. Our data also suggest that mitochondria outweigh the nucleus to overcome hypoxia-induced drug resistance. However, we could not fully exclude the possibility that nucleus has crosstalk with mitochondria in TCC cells for the reduction of cisplatin-induced apoptosis during hypoxia.

In conclusion, the present study shows that hypoxia induces drug resistance through modulation of the antitumor redox response, which results in mitigation of oxidative stress-induced mitochondrial damage, including mtDNA damage.

Declaration of competing interest

The authors declare that they have no competing interests.

Author contributions

Contributed to conception or design: MCK and YK. Contributed to the acquisition, analysis, or interpretation of the data: MCK, SH, NYK, YY, and YK. All authors read and approved the final manuscript.

Institutional review board statement

Not applicable.

Informed consent statement

Not applicable.

Data availability statement

The datasets used or analyzed during the current study are available from the corresponding author upon reasonable request.

References

[1] Hockel M, Vaupel P. Tumor hypoxia: definitions and current clinical, biologic, and molecular aspects. *J Natl Cancer Inst* 2001;**93**:266–76.

[2] Vaupel P, Mayer A. Hypoxia in cancer: significance and impact on clinical outcome. *Cancer Metastasis Rev* 2007;**26**:225–39.

[3] Cosse J-P, Michiels C. Tumour hypoxia affects the responsiveness of cancer cells to chemotherapy and promotes cancer progression. *Anticancer Agents Med Chem* 2008;**8**:790–7.

[4] Rohwer N, Cramer T. Hypoxia-mediated drug resistance: novel insights on the functional interaction of HIFs and cell death pathways. *Drug Resist Updat* 2011;**14**:191–201.

[5] Doktorova H, Hrabeta J, Khalil MA, Eckschlager T. Hypoxia-induced chemoresistance in cancer cells: The role of not only HIF-1. *Biomedical Papers of the Medical Faculty of the University Palacky* 2015;**159**:166–77.

[6] Richters A, Aben KK, Kiemeney LA. The global burden of urinary bladder cancer: an update. *World J Urol* 2020;**38**:1895–904.

[7] Siegel R, Miller K, Jemal A. Cancer statistics, 2020, 70; 2020. p. 7–30. Editor (ed)^(eds): City.

[8] Lenis AT, Lec PM, Chamie K. Bladder Cancer: A Review. *JAMA* 2020;**324**:1980–91.

[9] Massari F, Santoni M, Ciccarese C, Brunelli M, Conti A, Santini D, Montironi R, Cascinu S, Tortora G. Emerging concepts on drug resistance in bladder cancer: Implications for future strategies. *Crit Rev Oncol Hematol* 2015;**96**:81–90.

[10] Theodoropoulos VE, Lazaris AC, Sofras F, Gerzelis I, Tsoukala V, Ghikonti I, Manikas K, Kastriotis I. Hypoxia-inducible factor 1α expression correlates with angiogenesis and unfavorable prognosis in bladder cancer. *Eur Urol* 2004;**46**:200–8.

[11] Luo J, Lou Z, Zheng J. Targeted regulation by ROCK2 on bladder carcinoma via Wnt signaling under hypoxia. *Cancer Biomarkers* 2019;**24**:109–16.

[12] Tsui K-H, Hou C-P, Chang K-S, Lin Y-H, Feng T-H, Chen C-C, Shin Y-S, Juang H-H. Metallothionein 3 is a hypoxia-upregulated oncogene enhancing cell invasion and tumorigenesis in human bladder carcinoma cells. *Int J Mol Sci* 2019;**20**:980.

[13] Wallace DC. Mitochondria and cancer. *Nat Rev Cancer* 2012;**12**:685–98.

[14] Attardi G, Schatz G. Biogenesis of mitochondria. *Annu Rev Cell Biol* 1988;**4**:289–331.

[15] Kwong JQ, Henning MS, Starkov AA, Manfredi G. The mitochondrial respiratory chain is a modulator of apoptosis. *J Cell Biol* 2007;**179**:1163–77.

[16] Fulda S, Galluzzi L, Kroemer G. Targeting mitochondria for cancer therapy. *Nat Rev Drug Discovery* 2010;**9**:447–64.

[17] Yu M, Ozaki T, Sun D, Xing H, Wei B, An J, Yang J, Gao Y, Liu S, Kong C. HIF-1α-dependent miR-424 induction confers cisplatin resistance on bladder cancer cells through down-regulation of pro-apoptotic UNC5B and SIRT4. *J Exp Clin Cancer Res* 2020;**39**:1–13.

[18] Cho HJ, Kim JK, Kim KD, Yoon HK, Cho M-Y, Park YP, Jeon JH, Lee ES, Byun S-S, Lim HM. Upregulation of Bcl-2 is associated with cisplatin-resistance via inhibition of Bax translocation in human bladder cancer cells. *Cancer Lett* 2006;**237**:56–66.

[19] Kim M-C, Hwang S-H, Kim N-Y, Lee H-S, Ji S, Yang Y, Kim Y. Hypoxia promotes acquisition of aggressive phenotypes in human malignant mesothelioma. *BMC Cancer* 2018;**18**:819.

[20] Mutlu AG. Measuring of DNA damage by quantitative PCR. *Mutlu AG* 2012:283–4.

[21] Hashiguchi K, Zhang-Akiyama Q-M. Establishment of human cell lines lacking mitochondrial DNA. Springer; 2009. p. 383–91.

[22] Morris JK. A formaldehyde glutaraldehyde fixative of high osmolality for use in electron microscopy. *J Cell Biol* 1965;**27**:137–9.

[23] van Zandwijk N, Clarke C, Henderson D, Musk AW, Fong K, Nowak A, Loneragan R, McCaughan B, Boyer M, Feigen M. Guidelines for the diagnosis and treatment of malignant pleural mesothelioma. *Journal of Thoracic Disease* 2013;**5**:E254–307.

[24] Huber HJ, Dussmann H, Kilbride SM, Rehm M, Prehn JH. Glucose metabolism determines resistance of cancer cells to bioenergetic crisis after cytochrome-c release. *Mol Syst Biol* 2011;**7**:470.

[25] Lenaz G. Role of mitochondria in oxidative stress and ageing. *Biochimica et Biophysica Acta-Bioenergetics* 1998;**1366**:53–67.

[26] Savi A, Incerti E, Fallanca F, Bettinardi V, Rossetti F, Monterisi C, Compierchio A, Negri G, Zannini P, Gianolli L. First evaluation of PET-based human biodistribution and dosimetry of 18F-FAZA, a tracer for imaging tumor hypoxia. *J Nucl Med* 2017;**58**:1224–9.

[27] Nakanishi K, Hiroi S, Tominaga S, Aida S, Kasamatsu H, Matsuyama S, Matsuyama T, Kawai T. Expression of hypoxia-inducible factor-1α protein predicts survival in patients with transitional cell carcinoma of the upper urinary tract. *Clin Cancer Res* 2005;**11**:2583–90.

[28] Peixoto A, Fernandes E, Gaiteiro C, Lima L, Azevedo R, Soares J, Cotton S, Parreira B, Neves M, Amaro T. Hypoxia enhances the malignant nature of bladder cancer cells and concomitantly antagonizes protein O-glycosylation extension. *Oncotarget* 2016;**7**:63138.

[29] Zhuo M, Gorgun FM, Tyler DS, Englander EW. Hypoxia potentiates the capacity of melanoma cells to evade cisplatin and doxorubicin cytotoxicity via glycolytic shift. *FEBS Open Bio* 2020;**10**:789–801.

[30] Shin DH, Choi Y-J, Park J-W. SIRT1 and AMPK mediate hypoxia-induced resistance of non-small cell lung cancers to cisplatin and doxorubicin. *Cancer Res* 2013;**74**:298–308.

[31] Wang J, Biju MP, Wang M-H, Haase VH, Dong Z. Cytoprotective effects of hypoxia against cisplatin-induced tubular cell apoptosis: involvement of mitochondrial inhibition and p53 suppression. *J Am Soc Nephrol* 2006;**17**:1875–85.

[32] Papandreou I, Cairns RA, Fontana L, Lim AL, Denko NC. HIF-1 mediates adaptation to hypoxia by actively downregulating mitochondrial oxygen consumption. *Cell Metab* 2006;**3**:187–97.

[33] Geoghegan F, Buckland RJ, Rogers ET, Khalifa K, O'Connor EB, Rooney MF, Behnam-Motlagh P, Nilsson TK, Grankvist K, Porter RK. Bioenergetics of acquired cisplatin resistant H1299 non-small cell lung cancer and P31 mesothelioma cells. *Oncotarget* 2017;**8**:94711–25.

[34] Hirama M, Isonishi S, Yasuda M, Ishikawa H. Characterization of mitochondria in cisplatin-resistant human ovarian carcinoma cells. *Oncol Rep* 2006;**16**:997–1002.

[35] Cao J, Liu Y, Jia L, Zhou H-M, Kong Y, Yang G, Jiang L-P, Li Q-J, Zhong L-F. Curcumin induces apoptosis through mitochondrial hyperpolarization and mtDNA damage in human hepatoma G2 cells. *Free Radic Biol Med* 2007;**43**:968–75.

[36] Liang X-J, Finkel T, Shen D-W, Yin J-J, Aszalos A, Gottesman MM. SIRT1 contributes in part to cisplatin resistance in cancer cells by altering mitochondrial metabolism. *Mol Cancer Res* 2008;**6**:1499–506.

[37] Forkink M, Manjeri GR, Liemburg-Apers DC, Nibbeling E, Blanchard M, Wojtala A, Smeitink JA, Wieckowski MR, Willems PH, Koopman WJ. Mitochondrial hyperpolarization during chronic complex I inhibition is sustained by low activity of complex II, III, IV and V. *Biochimica et Biophysica Acta (BBA)-Bioenergetics* 2014;**1837**:1247–56.

[38] Okamoto A, Sumi C, Tanaka H, Kusunoki M, Iwai T, Nishi K, Matsuo Y, Harada H, Takenaga K, Bono H. HIF-1-mediated suppression of mitochondria electron transport chain function confers resistance to lidocaine-induced cell death. *Sci Rep* 2017;**7**:3816.

[39] Cho K, Shin H-W, Kim Y-I, Cho C-H, Chun Y-S, Kim T-Y, Park J-W. Mad1 mediates hypoxia-induced doxorubicin resistance in colon cancer cells by inhibiting mitochondrial function. *Free Radic Biol Med* 2013;**60**:201–10.

[40] Oliva CR, Moellering DR, Gillespie GY, Griguer CE. Acquisition of chemoresistance in gliomas is associated with increased mitochondrial coupling and decreased ROS production. *PLoS One* 2011;**6**:e24665.

[41] Li P, Zhang D, Shen L, Dong K, Wu M, Ou Z, Shi D. Redox homeostasis protects mitochondria through accelerating ROS conversion to enhance hypoxia resistance in cancer cells. *Sci Rep* 2016;**6**:22831.

[42] Zorov DB, Juhaszova M, Sollott SJ. Mitochondrial ROS-induced ROS release: an update and review. *Biochimica et Biophysica Acta (BBA)-Bioenergetics* 2006;**1757**:509–17.

[43] Waypa GB, Marks JD, Guzy R, Mungai PT, Schriewer J, Dokic D, Schumacker PT. Hypoxia triggers subcellular compartment redox signaling in vascular smooth muscle cells. *Circ Res* 2010;**106**:526–35.

[44] Fuhrmann DC, Brüne B. Mitochondrial composition and function under the control of hypoxia. *Redox Biol* 2017;**12**:208–15.

[45] DeHaan C, Habibi-Nazhad B, Yan E, Salloum N, Parliament M, Allalunis-Turner J. Mutation in mitochondrial complex I ND6 subunit is associated with defective response to hypoxia in human glioma cells. *Mol Cancer* 2004;**3**:19.

[46] Stiburek L, Cesnekova J, Kostkova O, Fornuskova D, Vinsova K, Wenchich L, Houstek J, Zeman J. YME1L controls the accumulation of respiratory chain

subunits and is required for apoptotic resistance, cristae morphogenesis, and cell proliferation. *Mol Biol Cell* 2012;**23**:1010–23.

[47] Kulikov AV, Vdovin AS, Zhivotovsky B, Gogvadze V. Targeting mitochondria by α-tocopheryl succinate overcomes hypoxia-mediated tumor cell resistance to treatment. *Cell Mol Life Sci* 2014;**71**:2325–33.

[48] Marrache S, Pathak RK, Dhar S. Detouring of cisplatin to access mitochondrial genome for overcoming resistance. *Proc Natl Acad Sci* 2014;**111**:10444–9.

[49] Wen S, Zhu D, Huang P. Targeting cancer cell mitochondria as a therapeutic approach. *Future Medicinal Chemistry* 2013;**5**:53–67.